LAWRENCE
LIVERMORE
NATIONAL
LABORATORY

LLNL-JRNL-641059

NMR Investigations of Network Formation and Motional Dynamics in Well-Defined Model Poly(dimethylsiloxane) Elastomers

J. P. Lewicki, S. J. Harley, C. Bell, J. A. Finnie, M. Ashmore, R. S. Maxwell

July 17, 2013

ACS Symposium Series

Disclaimer

NMR Investigations of Network Formation and Motional Dynamics in Well-Defined Model Poly(dimethylsiloxane) Elastomers

James P. Lewicki[1*], Stephen J. Harley[1], Jasmine A. Finnie[1], Michael Ashmore, Crystal Bell and Robert S. Maxwell[1]

[1]Lawrence Livermore National Laboratory, 7000 East Ave. Livermore, CA.

In this work, results of a study to optimize the structure of a series of model PDMS networks are reported. The study utilized ^{1}H Magic Angle Spinning (MAS), Magic Sandwich Echo (MSE) NMR methods and equilibrium solvent uptake analysis. The influence of inter-crosslink molar mass, vinyl to silane ratio and Pt chelation effects on the dynamics of network formation have been studied using low field NMR methodologies in real time. These comparatively simple solid-state NMR methodologies can be used to study the dynamics of network formation and the relationship between the chemical identity of key structural components and the final network structure of a silicone elastomer.

Introduction

Crosslinked Poly(dimethylsiloxane) (PDMS), elastomeric networks are an academically and technologically relevant sub-group of polysiloxane based materials, having wide-spread application in a large number of diverse technological, commercial and research areas (*1,2,3,4*). Simple end-linked,

unfilled, condensation, addition or peroxy- cured PDMS networks typically exhibit poor mechanical properties and are of limited use as engineering elastomers (*5*). It is understood that in order to obtain the desired combinations of mechanical, physical and chemical properties for a specific real world application, the silicone formulation must, in fact, be comprised of complex multi-component systems - incorporating multi-modal distributions of chain lengths, varied crosslink topologies/densities, chemically modified free chain ends, non-stoichiometric excesses of reactive moieties, and often large volume fractions of a variety of reactive and/or passive filler materials. The extensive modification process often results in a material with empirically tuned physical properties but is characterized by a highly complex and often poorly defined network structure (see **Figure 1**).

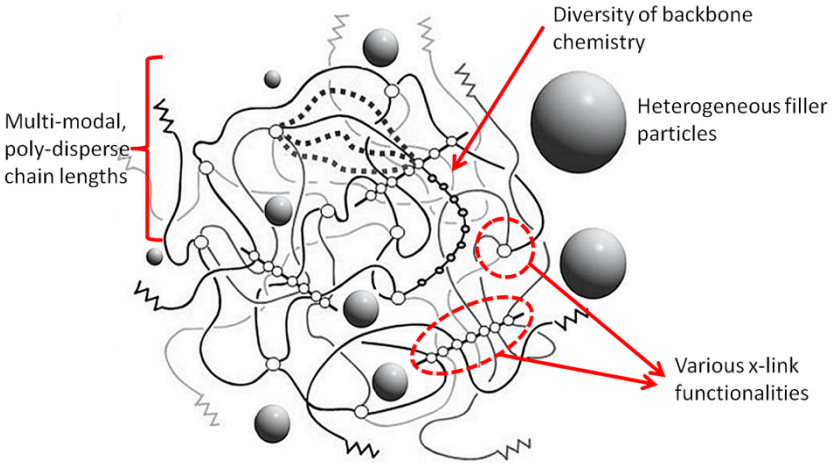

Figure 1. Illustration of the main contributory factors that define the complex structural architecture of an engineering silicone elastomer.

The physical, chemical properties and hence the performance of a silicone elastomer are governed by this underlying network structure. Therefore, in order to make accurate assessments and predictions of a materials performance and lifetime over a broad range of environmental conditions and to design materials with better defined, enhanced chemical and physical properties (*6,7*), we must improve our understanding of the relationship between the underlying network architecture and macro-scale materials behavior.

In the past there has been a reliance on purely empirical additive methodologies in defining structure-property relationships in silicone elastomers for the prediction of materials performance (*8,9,10*). And beyond the most

coarse grain information, the specifics of the network architecture have historically been largely ignored.

Today, there is a need to move beyond basic bulk and qualitative approaches and attempt to build a firm analytical model that links complex structural architectures over a broad range of size scales, which may be used for predicting materials performance and lifetimes. The practical realization of this goal requires a multi-scale effort encompassing the study of both model and commercial materials, using a broad range of interrogative analytical methodologies (*11,12,13*), computational modeling (*14,15*) and long term aging studies for model validation (*16*). In this article, we focus on analytical approaches towards the development of well-defined model network materials for the study of structure-property relationships in silicone systems.

Analytical Methodologies for the Analysis of Intractable Silicone Networks

Silicone elastomers are chemically crosslinked networks with an effective infinite molecular weight and are as such, insoluble. Furthermore, the high filler loadings and crosslink-densities - typically encountered in the majority of silicone engineering elastomers - render these networks intractable with respect to many commonly employed polymer characterization techniques. Consequently, high-fidelity structural information may only be accessed through means of solid-state spectroscopies or destructive analysis methods and is often non-trivial to obtain. In spite of this intractability, much progress has been made towards understanding structure-property relationships in complex siloxanes over the last three decades. Notably, Mark et al. have made extensive study of the association between network functionality, modality, filler content and the bulk mechanical/rheological properties of model silicone networks (*17,18,19*). Clarson et al. have studied modification of silicone based materials with a range of fillers and other physical property modifiers in great depth (*20*). Notably, Cohen-Addad made early use of solid and solution state NMR methodologies for the study of the properties of silicone melts, gels and silica-silicone systems (*21*)

Destructive, non-spectroscopic methods are also available that may be developed to probe network structure in intractable silicone networks. A worthy example is Thermal Analysis (A thorough review of which has been published by Wunderlich (*22*)). Thermal analysis techniques such as Pyrolytic analysis and gravimetry have been used extensively for the analysis of 'unknown' polymeric materials for many years (*23,24,25,26*). The temperature at which a polymeric material degrades, the mechanism and the products of the thermal degradation are all a function of its underlying chemical structure and even physical morphology. Different polymeric materials can therefore be 'fingerprinted' by their thermal or thermo-oxidative degradation behavior. It is

now becoming apparent that the same holds true for silicone based materials (*11*).

While there does indeed exist a range of approaches for the in-depth investigation of structure and properties of complex silicones, it is perhaps Nuclear Magnetic Resonance (NMR) that is uniquely suited in its ability as a family of techniques to probe the structure and properties of silicones: from an atomistic-molecular scale (high resolution chemical shift dependence), in terms of their dynamic physical structure (relaxometry) and at a micro/macroscopic scale (magnetic resonance imaging (MRI)). Over the last 2 decades solid-state Nuclear Magnetic Resonance (NMR) in particular has been shown extensively (*27,28,12*) to be a powerful tool for directly elucidating the chemical identity and network architecture of complex engineering siloxanes. Cohen-Addad (*29,30*), Charlesby (*31,32*), Saalwatcher (*33,34*), Maxwell (*35*) and others have made extensive use of solid-state NMR both as a method of determining the chemical content/makeup of the polymer backbone in commercial silicone formulations and as a tool for probing segmental dynamics of silicone networks in the solid state by utilizing spin echo and novel multiple quantum NMR methodologies (*36,13*).

In this paper, a range of methodologies are applied to the analytical optimization, determination of cure kinetics and final network structure in model, end-linked addition cured PDMS networks. By utilizing a range of solid state NMR methodologies in combination with equilibrium solvent uptake measurements, the influence of inter-chain molar mass, functional group stoichiometry and concentration on both the dynamic cure behavior and final structure of a series of well-defined model networks have been investigated. The results of these studies yield new insight into the complexities of addition cured silicone networks and will aid in the development of a multi-scaled approach towards the predictive modeling of silicone lifetimes and behavior.

Experimental

Materials

All Poly(dimethylsiloxane) (PDMS) polymers, tetrakis-dimethyl-methoxysilane (TKSIL) crosslinker, Platinum di-vinyl-methylsiloxane catalyst used in this study were obtained from Gelest Inc.

Synthesis of Model Networks

End-linked, tetra-functionally crosslinked 'model' networks were synthesized via a organoplatinum mediated hydrosilation reaction between vinyl terminated poly(dimethylsiloxane) (PDMS) and a organo-tetra-silane crosslinker to form network elastomers with average inter-crosslink chain lengths of 6, 28 and 115.5 kg mol^{-1}. Each model system was formulated in the following manner: 55 Grams of a given vinyl terminated PDMS (6, 28 or 115.5 kg mol^{-1}) was combined with a quantity of TKSIL crosslinker corresponding to a silane to vinyl ratio of 0.5:1 to 4:1 in the presence of 40 ppm of a Pt di-vinyl-methyl-siloxane complex and mixed for 30 seconds using a Flactek^{tm} Speedmixer off-axis centrifugal mixer at a rate of 2500 rpm. The mixed resin was then poured into a 6 by 6 inch by 2 mm deep ASTM D3182 mold and allowed to cure for 12 hours at room temperature. The formed elastomer was subsequently removed from the mold and post-cured for an additional 24 hours at 80°C under vacuum. One inch square samples were cut from the original sheet, swollen in 500 ml of spectroscopy grade toluene for 12 hours to remove any unreacted material or small molecule impurities and then re-dried under vacuum at 80°C for a further 24 hours. This process was repeated for each chain length and silane ratio variant to yield a matrix of 45 systems - details of which are given in **Table 1**.

Table 1. Model end-linked PDMS synthesized networks

Sample code	Molar mass PDMS /$gmol^{-1}$	Silane to Vinyl ratio	Physical State	Sample code	Molar mass PDMS /$gmol^{-1}$	Silane to Vinyl ratio	Physical State
11_A	6000	0.5	No gel	13_K	28,000	3	Stiff gel
11_B	6000	0.75	Partial gel	13_L	28,000	3.25	Partial gel
11_C	6000	1	Partial gel	13_M	28,000	3.5	Partial gel
11_D	6000	1.25	Gel	13_N	28,000	3.75	Partial gel
11_E	6000	1.5	Gel	13_O	28,000	4	Partial gel
11_F	6000	1.75	Stiff gel	17_A	115,000	0.5	Partial gel
11_G	6000	2	Gel	17_B	115,000	0.75	Partial gel
11_H	6000	2.25	Partial gel	17_C	115,000	1	Partial gel
11_I	6000	2.5	Partial gel	17_D	115,000	1.25	Gel
11_J	6000	2.75	Partial gel	17_E	115,000	1.5	Gel
11_K	6000	3	Partial gel	17_F	115,000	1.75	Stiff gel
11_L	6000	3.25	Partial gel	17_G	115,000	2	Stiff gel
11_M	6000	3.5	Partial gel	17_H	115,000	2.25	Gel
11_N	6000	3.75	No gel	17_I	115,000	2.5	Gel
11_O	6000	4	No gel	17_J	115,000	2.75	Gel

Sample code	Molar mass PDMS /gmol^{-1}	Silane to Vinyl ratio	Physical State	Sample code	Molar mass PDMS /gmol^{-1}	Silane to Vinyl ratio	Physical State
13_A	28,000	0.5	No gel	17_K	115,000	3	Gel
13_B	28,000	0.75	No gel	17_L	115,000	3.25	Gel
13_C	28,000	1	Partial gel	17_M	115,000	3.5	Partial gel
13_D	28,000	1.25	Partial gel	17_N	115,000	3.75	Partial gel
13_E	28,000	1.5	Gel	17_O	115,000	4	Partial gel
13_F	28,000	1.75	Stiff gel	-	-	-	-
13_G	28,000	2	Stiff gel	-	-	-	-
13_H	28,000	2.25	Gel	-	-	-	-
13_I	28,000	2.5	Gel	-	-	-	-
13_J	28,000	2.75	Stiff gel	-	-	-	-

NMR Analysis

High-Field Magic Angle Spinning (MAS) NMR experiments were performed on a Bruker Avance spectrometer operating with a proton Larmor frequency of 400.13 MHz, using a Bruker MAS probe configured for 4 mm (o.d.) rotors. ~500 mg Samples were powdered and packed into silicon nitride rotors. Samples were spun at 15 kHz and ninety degree pulse lengths of τ_p = 8 μs and recycle delays of 1.4 seconds were used. The spectra were referenced with respect to tetramethylsilane (0 ppm).

Low-field solid-state NMR studies were performed on a Bruker Minispec™ spectrometer at 37±0.1°C under static conditions. Ninety degree pulse lengths of τ_p = 2.25 μs and recycle delays of 15 seconds were used. Highly rigid domains relax more rapidly than the dead time of the probe. Therefore, to regain information that may be lost during this time, a special form of refocusing sequence known as the Magic Sandwich Echo (MSE) (*37*) was employed. With MSE, near quantitative refocusing of fast relaxing components is achieved where subsequent application of a Carr-Purcell-Meiboom-Gill (CPMG) train removes the effects of magnetic field inhomogeneities (*38*). This technique is highly effective at obtaining free induction decays (FIDs) that are representative of large distributions of relaxation times.

The application of the MSE yields an FID that is a superposition of decaying exponentials whose amplitudes and time constants are representative of unique molecular motion distributions within the material. However, the extraction of this information is mathematically non-trivial (*39,40*). Direct non-linear regression to an unknown sum of exponentials is possible yet impractical

as it requires a priori knowledge of the relaxation behavior of the material of study. Ideally, a mathematical transform is sought to de-convolute the time domain data into a spectral domain - much akin to a fast Fourier transform. Such a spectral function can only be found upon solution of the Laplace integral equation (*41*) which is part of a more general class of Fredholm integral equations. Many algorithms exist to accomplish this transformation (including the fast Tikhonov regularization routines, CONTIN (*42*) and FTIKREG (*43*) that only vary in the method used to find the criteria for the regularization parameter.

In this work, all data was processed using the FTIKREG routine. It is important to note that the solution to the Laplace integral equation may depend continuously on the data (*44*) and may not be unique. To assure confidence in the obtained spectral function, samples were run in the spectrometer a total of three times in random order.

Equilibrium Solvent Uptake Analysis

Equilibrium solvent uptake analyses of the samples were performed using a 5:6 v/v toluene/acetone mixture at 29.5 °C as the swelling medium which provides theta conditions for the polymer chains. Samples of ~25 mg mass were swollen under these conditions for 48 h and triplicate samples of each system were swollen for statistical accuracy. The swollen samples were surface dried then weighed using a sensitive microbalance (Mettler Toledo) to an accuracy of $\pm 5 \times 10^{-7}$ grams. After measurement, the networks were un-swollen gradually in methanol then dried in a vacuum oven overnight at 80 °C. The samples were weighed again and these values were used to calculate both the mass of solvent uptake per gram for each sample and fraction soluble material extracted during the swelling process.

The average inter-crosslink chain density $\langle M_x \rangle$ was calculated from these data using the Flory-Hugins relationship (*45*) under equilibrium conditions, given in **Equation 1**.

$$< M_x >= \frac{-\rho_{poly} V_{m,solv} (c^{\frac{1}{3}} - \frac{c}{2})}{[\ln(1-c) + c + \chi c^2]} \qquad \textit{Equation 1}$$

Where ρ_{poly}= the density of the pure polymer, ρ_{solv} = solvent density $V_{m,solv}$= the molar volume of the solvent and χ = the chi parameter of the solvent (0.5 for a theta solvent). *'C' = the relative concentration and is given by* ***Equation 2.***

$$c = \frac{W_0}{\rho_{poly} V} \qquad \textit{Equation 2}$$

Where W_0=the initial polymer mass and V = volume of swollen polymer.

Results and Discussion

Optimization of model networks

Organoplatinum complexes such as Karstedt's catalyst are an effective and well established class of homogenous catalysts for hydrosilylation reactions (*46*). With Karstedt's catalysts and related variants, Pt(0) is chelated by bridged vinyl-siloxane ligands. The active complex, during a hydrosilation process relies on the transfer of the silane to the Pt(0) center followed by a subsequent change in the ligand complexion number and complexation with a the double bond of interest which is turn, activated towards addition of ~Si-H to form the addition product as shown in **Figure 2**.

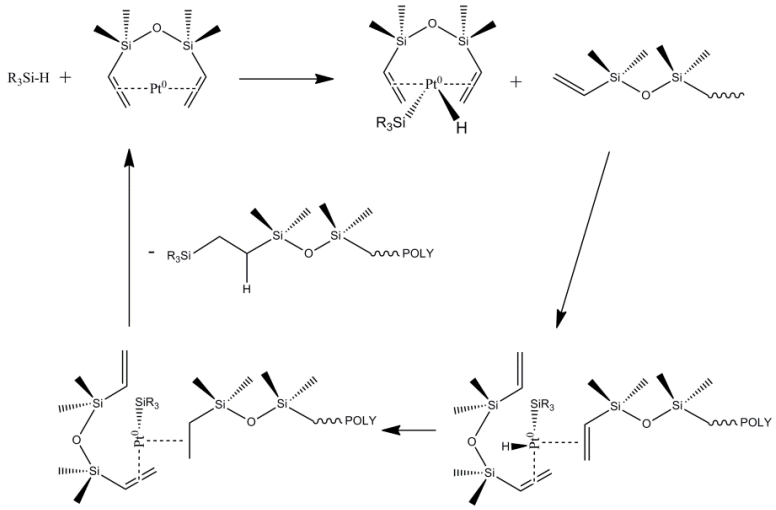

Figure 2. A basic, generalized scheme for the Pt mediated hydrosilation of a vinyl end-group on a PDMS polymer chain. Pt(0) is stabilized in a chelated state through complexation with a vinyl silane. Addition proceeds though a multi-stage mechanism involving 1) hydrogen transfer to the Pt center, 2) complexation with a vinyl and a n-1 reduction in ligand number of the Pt complex, 3) silane addition to the double bond and 4) regeneration of the original Pt complex.

Vinyl terminated PDMS resins can therefore be readily crosslinked in the presence of low levels of a Pt(0) organoplatinum complex (1-50 ppm). And although such organoplatinum complexes are considered to be highly active for room temperature vulcanization processes, these reactions are also highly temperature dependent. Furthermore, during network formation, they do not always proceed stoichiometrically with respect to vinyl-silane ratio. When attempting to form 'model' materials with idealized network structures it is therefore important to take into account these features of Pt mediated hydrosilylation. To that end, a simple tetra-functional end-linked network architecture has been selected, based on a TKSIL silane cross-linker and three different molar mass bis-vinyl terminated PDMS polymers of molar mass 6, 28 and 115.5 kg Mol^{-1} – representing network chain lengths below, above and very highly above the critical chain entanglement length of PDMS (~12 kg mol^{-1}) - named Models 11, 13 and 17 respectively. In order to experimentally determine the optimum silane:vinyl ratio for each model system, a series of variants of each was formulated with a varying silane:vinyl ratio - from 0.5:1 to 4:1 (see **Table 1**). Equilibrium solvent uptake measurements were carried out on each variant, their x-link densities and percentage sol-fractions were determined. The results of which are shown in **Figures 3-5.**

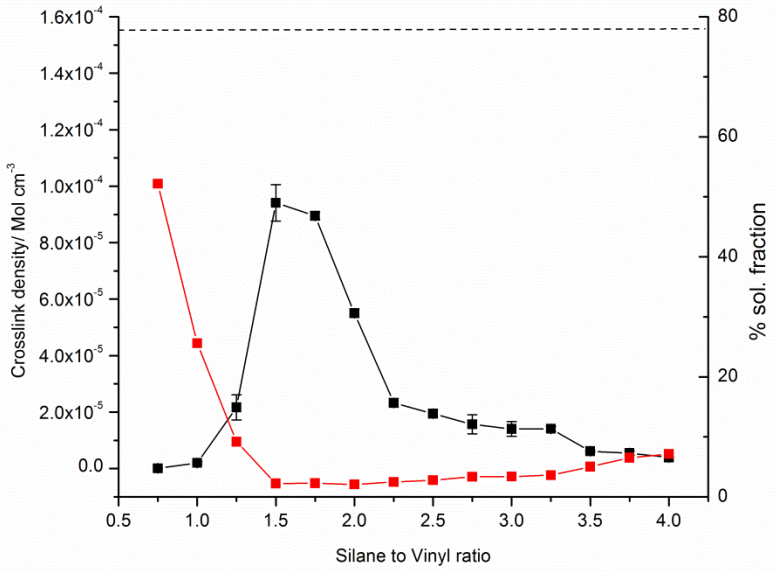

Figure 3. Equilibrium solvent uptake data for 'Model 11' with a silane ratio varied from 0.75 to 4. Left axis depicts crosslink density as a function of

silane:vinyl ratio (black line), right axis the % extracted sol. fraction as a function of silane:vinyl ratio (red line). The dashed horizontal line represents the theoretical maximun crosslink density achievable from the complete conversion of a 6 kg mol^{-1} tetra-functional end-linked network. Note that the maximum experimental crosslink density is somewhat lower than the theoretical value for Model 11 and that this value and the minimum sol. fraction value correspond to a silane:vinyl ratio of ~1.75:1.

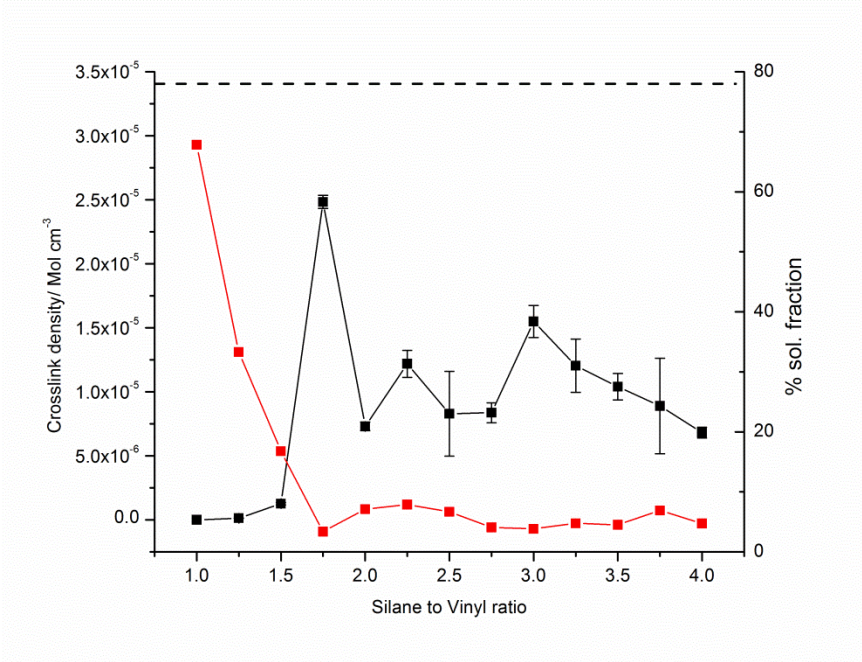

Figure 4. Equilibrium solvent uptake data for 'Model 13' with a silane ratio varied from 1 to 4. Left axis depicts crosslink density as a function of silane:vinyl ratio (black line), right axis the % extracted sol. fraction as a function of silane:vinyl ratio (red line). The dashed horizontal line represents the theoretical maximum crosslink density. Note again that the maximum experimental crosslink density is somewhat lower than the theoretical value for Model 13 and that this value and the minimum sol. fraction value correspond to a silane:vinyl ratio of 1.75:1.

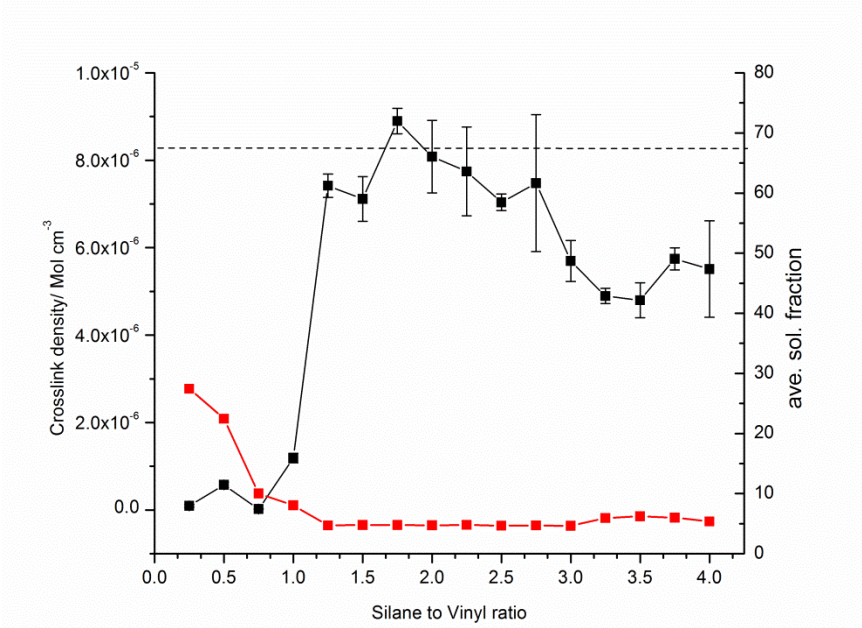

Figure 5. Equilibrium solvent uptake data for 'Model 17' with a silane ratio varied from 0.25 to 4. Left axis depicts crosslink density as a function of silane:vinyl ratio (black line), right axis % extracted sol. fraction as a function of silane:vinyl ratio (red line). The dashed horizontal line represents the theoretical maximum crosslink density. In contrast to Models 11 and & 13, the maximum experimental crosslink density is marginally higher than the theoretical value for Model 17. The % extractables are also correspondingly lower due to the decreased mass fraction of crosslinker present, however once again the maximum experimental crosslink density value corresponds to a silane:vinyl ratio of 1.75:1.

From the data shown in **Figures 3-5** it can be observed that irrespective of chain length, Models 11-13 reach a maximum crosslink density at a silane to vinyl molar ratio of ~1.75:1. Therefore it appears that in order to achieve close to full conversion and maximum network density in this class of end-linked network, a moderate silane excess is required. This ratio may at first appear counter intuitive, however if we consider that there are 4 moles of silane per TKSIL molecule and 2 moles of vinyl per PDMS chain, then the stoichiometric (1:1) level of silane, numerically provides only ½ the number of TKSIL molecules to PDMS chains. However, at a 1.75:1 molar ratio there is almost a 1:1 numerical balance of TKSIL to polymer molecules and from the solvent uptake data it appears that having near to 1:1 molar balance between TKSIL and

PDMS molecules, rather than a stoichiometric balance between silane and vinyl groups is essential for the formation of a fully dense network. This silane rich, non-stoichiometric environment is illustrated graphically in **Figure 6**.

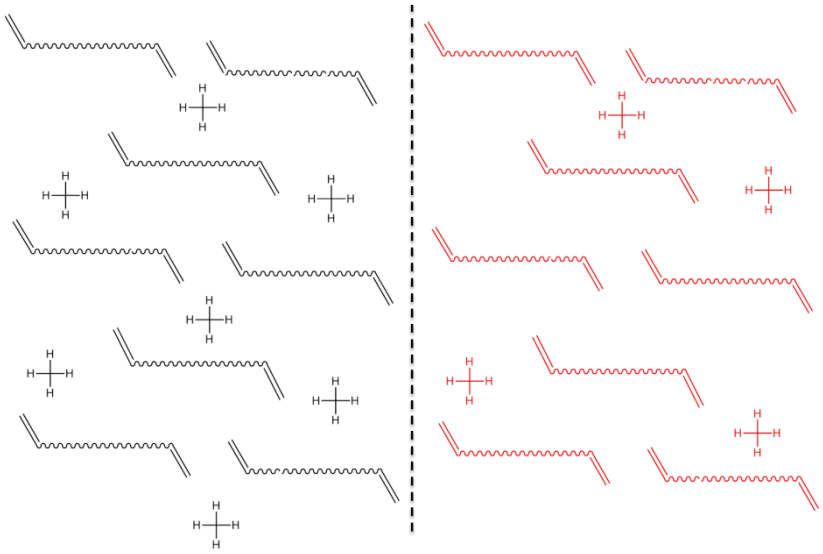

Figure 6. Illustration of the numerical difference between (left) a near to 1:1 Molar ratio of crosslinker molecules to polymer chains - as is the case with the optimized model networks and (right) a 1:1 molar ratio of silane to vinyl groups – which would be obtained from a stoichiometric calculation. Although a gross simplification of the network formation chemistry, this illustration highlights the fact that a ~1:1 ratio of x-linker to polymer is required per unit volume for the formation of a fully dense network.

Solvent uptake measurements provide evidence that the network formation process(es) taking place in these model systems are somewhat more complex than would at first be expected. The fact that a 1:1 silane to vinyl ratio does not result in the formation of a fully dense 'ideal' network structure even when driven thermally by an aggressive post-cure, suggests that other factors such as chain-end mobility, local spatial availability of reactive groups and catalyst immobilization/deactivation may influencing the ability of the precursors to form an ideal network structure. With these considerations in mind, we have employed solid-state NMR methodologies to attempt to further investigate the processes of network formation in each class of model system both as a function of silane:vinyl ratio and in real time.

In theory, the progress of the network formation reaction can be followed through direct NMR observations of the relative populations of silane and vinyl functional groups. Solution state experiments are not suited to the analysis of systems which undergo a melt to solid transition and are therefore subject to excessive line broadening and the loss of chemical shift resolution (*47*) as the reaction proceeds. Relatively simple solid state experiments, however, can be employed to negate these difficulties. Magic Angle Spinning (MAS) NMR is one such method which has been employed here and shown in **Figure 7** is a ^{1}H-MAS NMR spectrum of Model 11-C.

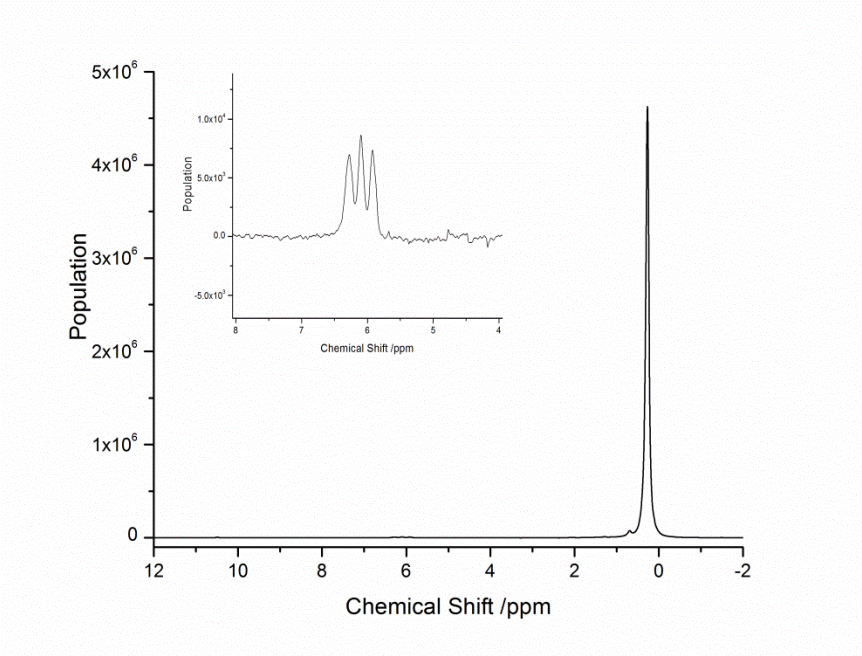

Figure 7. ^{1}H MAS NMR spectrum of a fully cured sample of Model 11-C. The main peak at 0.26ppm corresponds to the methyl protons of the PDMS backbone. Shown (inset) at 7.1ppm is the comparatively weak proton resonance from the residual vinyl end groups of model 11-C. Note that greater than 99% of the ^{1}H signal is resultant from the abundant methyl backbone protons. No silane peak was observed.

The ^{1}H NMR spectrum of Model 11-C (**Figure 7**) clearly shows that despite 11-C having a 1:1 silane to vinyl ratio and having undergone an extensive post-cure, it has an excess of vinyl groups present in the matrix and no detectable silane signal. This both aggress with the solvent uptake data and physical

appearance of the material, showing it to be a partially crosslinked gel. These data demonstrate that the silane addition reaction does not proceed quantitatively within these matrices.

While ^{1}H-MAS of the model systems can clearly resolve distinct chemical moieties within the crosslinked polymer matrix and has demonstrated that networks formed from 1:1 silane:vinyl ratio precursors actuality retain a significant vinyl excess, such direct detect methods are limited in sensitivity by the typical detection limits of NMR (>100's of mMolar) and the comparatively low abundance of protons corresponding to functional end groups of interest. Direct ^{1}H MAS methods are therefore generally capable of detecting comparatively large excesses of functional groups, and are not generally effective at following network reactions at high conversion levels.

Given the limitations of chemical shift resolved end-group analysis at low concentrations and high conversion levels, it is NMR relaxometry methodologies which have been utilized for the further study of network ideality and for real-time analysis of network formation in the model materials. Such methods - which measure characteristic relaxation times of observed nuclei [the spin lattice relaxation time (T_1), the transverse relaxation time (T_2), the residual dipolar coupling constant ($D_{<res>}$), etc (*48*)] related to the mobility of that nuclear spin population of interest - do not provide direct chemical speciation within a network but can yield effective information on the motional dynamics of a network elastomer (*[36]*). These methods have also been used to distinguish discrete populations of nuclei in differing motional environments (*49*).

For the analysis of the model silicone networks discussed here, comparatively simple and rapid low-field relaxometry techniques have been employed. These techniques are reliant on the re-focusing and measurement of ^{1}H T_2 values using a Magic Sandwich Echo (MSE) pulse sequence (see Experimental section) optimized for the model silicone networks. Our initial study using MSE, attempted to relate distributions of T_2 times to network ideality as a function of silane:vinyl ratio, the results of which are given in **Figure 8**.

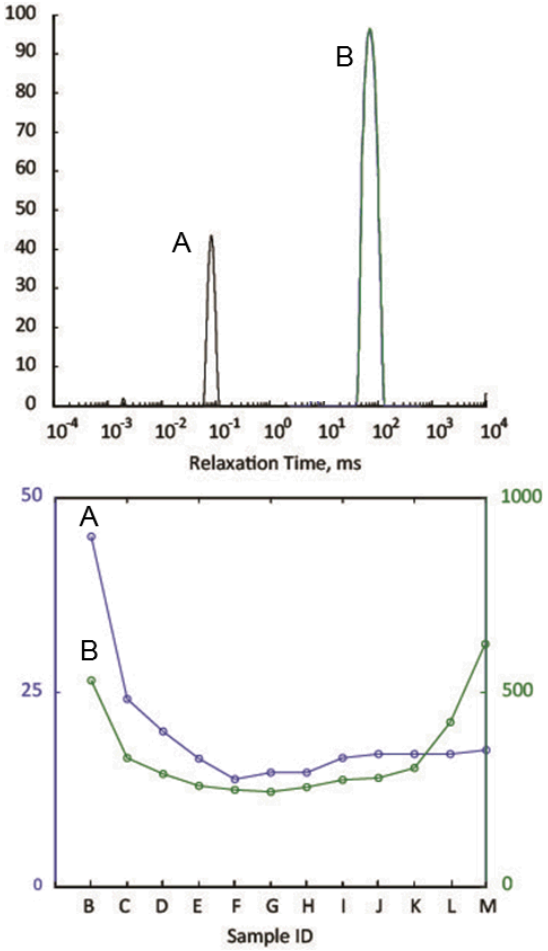

Figure 8. ^{1}H MSE NMR analysis of Models 13-B to 13-M. The upper plot shows the derived populations of protons having distinct relaxation times in this example, Sample 13-M. Two populations of protons having distinct relaxation times are considered which have been be related to system protons with differing mobilities, marked A and B. In the lower plot, the average T_2 values of these populations are plotted for systems 13-B to M, corresponding to silane:vinyl ratios of 0.75-3.5:1. Note that a convergence in relaxation times is observed around the 1.75:1 ratio.

The example shown in **Figure 8** demonstrates that the MSE technique can distinguish distinct populations of system protons within the model networks which have characteristic T_2 relaxation times. Given that T_2 can be broadly

related to mobility ($T_2 \propto$ 'proton mobility') within these networks, we can consider these populations to be representative of fractions of the polymeric system within different motional domains. What is significant is that the average relaxation times of these groups vary as a function of the network stoichiometry: at low and high silane ratios, components 'A' and 'B' have distinct distributions of relaxation times; however, as the stoichiometry approaches a ratio of 1.75:1 these distinct populations converge. These data demonstrate that on either side of the conversion curve, the networks are heterogeneous in their motional dynamics and have distributions of both comparatively 'rigid' gel type structure (A) and liquid like components (B) additionally, as these systems approach the fully dense 'ideal' network structure both of these components become less mobile and eventually become indistinguishable – an indication that a homogenous network structure has been approached.

Real-time analysis of network formation in optimized systems

Through the combination of equilibrium solvent uptake and NMR analysis of the model network formulations, it has been determined that the network structure of each given system reaches an optimum in terms of crosslink density and network homogeneity at a silane to vinyl ratio of 1.75:1- irrespective of the molar mass of the PDMS precursors. The dynamics of the network formation processes during the curing of these optimized systems (hereafter referred to as Models 11, 13 and 17) have been investigated using ^{1}H MSE NMR. For each given 'optimized' model variant, the curing behavior has been studied in real time and in-situ. 2 Gram batches of Models 11, 13 and 17 were formulated in 10mm NMR tubes and allowed to cure at 37 °C within the Spectrometer. During this time, MSE relaxometry measurements were made at regular intervals in order to track the change in T_2 for each system as a function of cure time. The extracted T_2 distributions for Model 13 as a function of cure time are shown in **Figure 9.** Shown in **Figure 10** is a plot of the amplitude of each relaxation curve as a function of cure time.

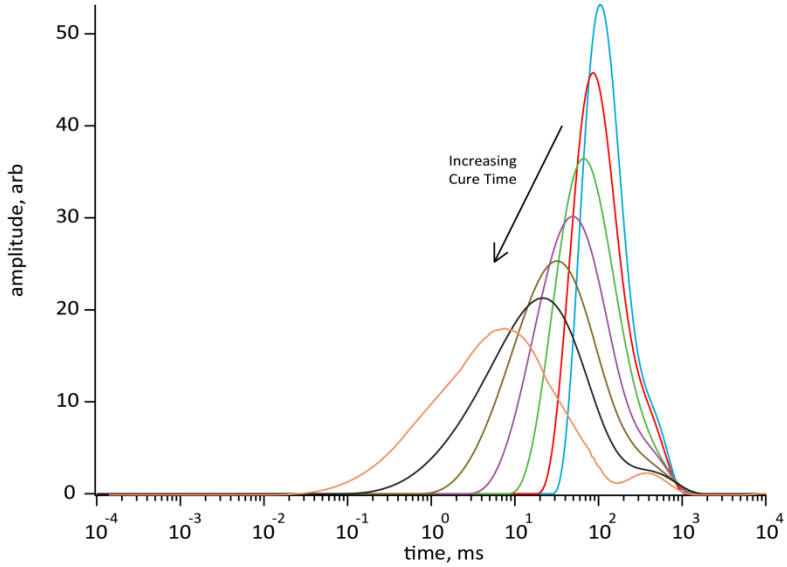

Figure 9. Derived T_2 distributions for optimized Model 13 as a function of cure time (0 – 40 min., 37°C). With increasing cure time, there is a progressive decrease in the amplitude and a broadening of the T_2 distribution, indicative of increasing motional constraint within the system as the system cures. Note that at long cure times, a highly mobile, slow relaxing component manifests itself.

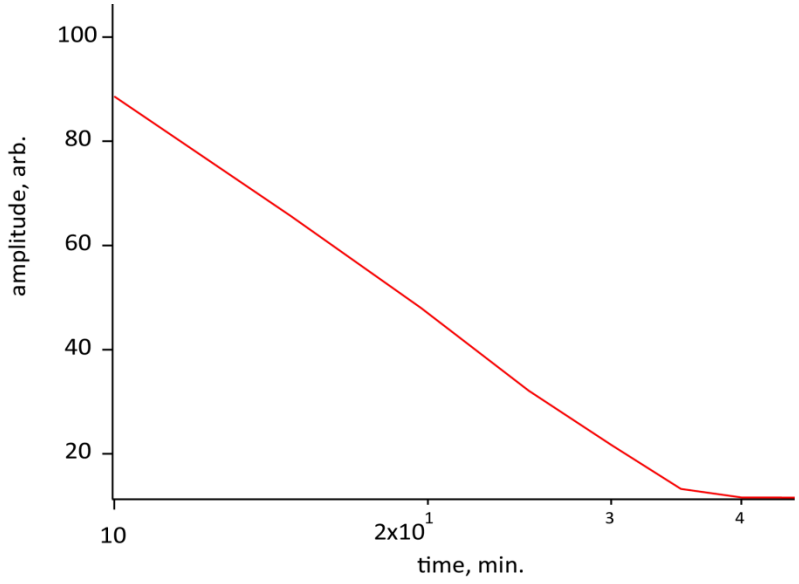

Figure 10. Derived relaxation amplitude as a function of cure time for the optimized Model 13. Note the decrease in amplitude of the relaxation curve follows a simple exponential decay process –consistent with the kinetics of a typical network formation process, the rate of which decreases exponentially as 100% conversion is approached.

The NMR analysis of the curing of Model 13 (**Figures 9&10**) clearly shows that the optimized system behaves in a manner consistent with the formation of a typical end-linked network. The cure rate is non-linear and decreases as a function of total cure time – owing to the decreasing availability of reactive functional groups and increasing viscosity as the network approaches high conversion levels. The appearance of a small yet distinct slowly relaxing component at long cure times has been attributed to the rapid motions of excess crosslinker and solvent species expelled from the network as it undergoes densification on curing. In general, from these data we can conclude that the 28 kg mol^{-1} model network formation process is similar in its cure kinetics to that of a typical thermoset network polymerization processes. If the starting molar mass of the PDMS resin is however increased significantly, with a corresponding decrease in the number of moles per unit volume of reactive groups (as is the case with Model 17) a differing cure behavior is observed. Shown in **Figures 11** & **12** are the extracted T_2 distributions for the optimized Model 17 and the amplitude of each relaxation curve as a function of cure time respectively.

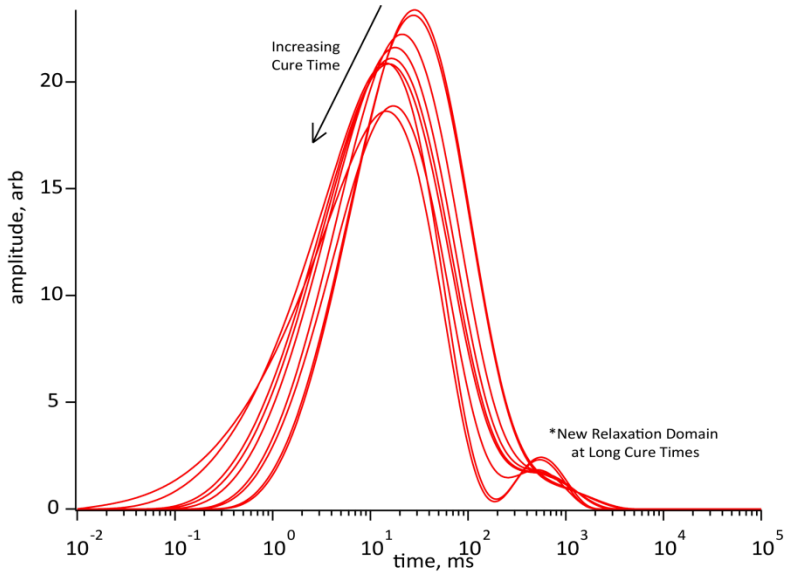

Figure 11. Derived T_2 distributions for optimized Model 17 as a function of cure time (0 – 4000 min., 37°C). In contrast with Model 13, the cure time of Model 17 is increased by 3 orders of magnitude and the distribution cures do not exhibit the same simple trend as a function of cure time. Note that at long cure times, there is once again a mobile, slow relaxing component present.

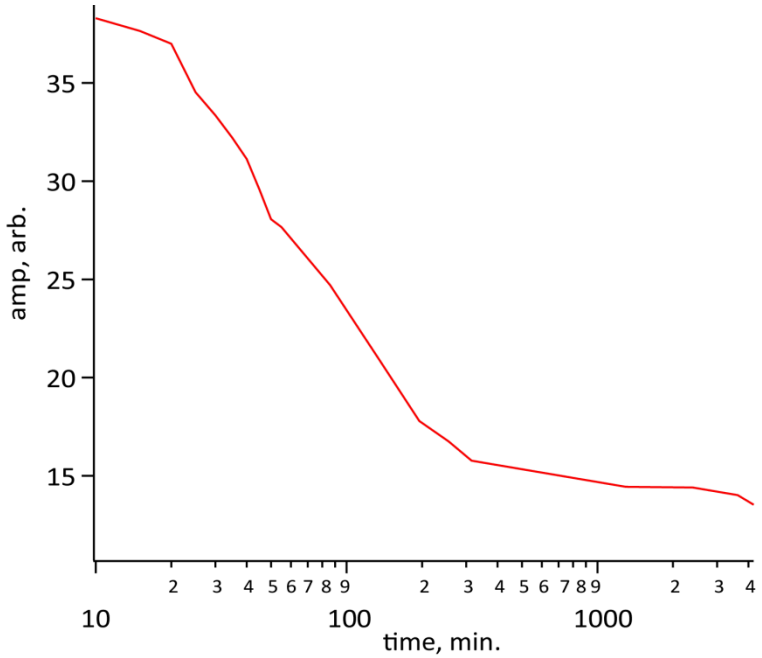

Figure 12. Derived relaxation amplitude as a function of cure time for the optimized Model 17. In this case at high initial molar masses, the decrease in amplitude of the relaxation curve does not follow a simple exponential decay process and the kinetics of the network forming process instead follow a higher order model.

In Model 17 the intercrosslink chain lengths are significantly greater than Model 13 and as such the initial melt viscosity of the formulation is much greater than that of Model 13. It also follows that the relative concentration of functional reactive groups is significantly lower with respect to Model 13. The practical consequence of these factors are that although the reaction proceeds, the cure time is greatly retarded and full conversion is only obtained at 37°C after ~4000 minutes. The results in **Figure 12** also clearly show that the overall network formation process no longer follows a simple exponential rate law and at these high viscosities and low functional group concentrations. Instead, the

silane addition network forming reaction follows a complex, higher order kinetic rate law. Simply increasing the molar mass of the linear precursor has a significant impact on the complexity of the network formation process.

At the other extreme lies Model 11, which has an average intercrosslink molar mass of ~6 kg mol^{-1} and correspondingly the highest relative concentration of vinyl groups of all three systems. Surprisingly, Model 11 did not achieve a full cure at room temperature. The optimized system was observed to partially gel at room temperature within ~2 minutes of the addition of the catalyst but was not observed to proceed further. Even samples left at room temperature for >1 month remained a partial gel and did not fully cure. Model 11 only achieves full network density after post-curing at elevated temperatures. As such, MSE analysis of the 'real-time' curing of Model 11 does not show any progressive trend in the amplitude of the measured T_2 distribution curves (see **Figure 13**) but instead shows evidence of the progressive in-growth of a very fast relaxing component (only partially captured in the NMR experiment – we will return to this later) as a function of cure time.

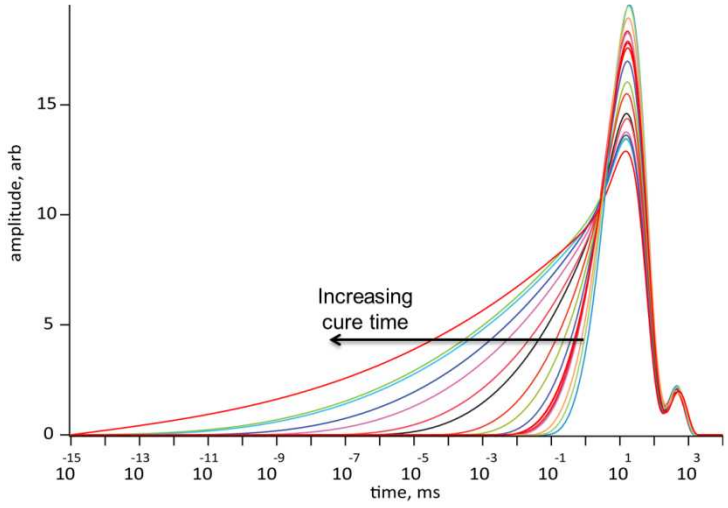

Figure 13. Derived T_2 distributions for optimized Model 11 as a function of 'cure' time (0 – 2600 min., 37°C). In stark contrast with Models 13 & 17, this low molar mass system effectively does not cure at room temperature. The system rapidly gels (not captured in this experiment) but will proceed no further at 37°C. The only clear trend is the progressive in-growth of a very fast relaxing component that was only partially captured in this experiment and as such manifests itself in this fit as a tail towards the left of the plot and not a true distribution.

The fact that Model 11 does not cure at moderate temperatures is significant. The comparatively high concentrations of reactive functional groups and low starting viscosities should lend themselves to a rapid cure. And indeed, the systems are observed to gel in less than 2 minutes. The reaction, however, did not proceed further at room temperature and required treatment at 80°C for extended time periods to drive the network formation process to completion. It is suggested that this anomalous cure behavior is a consequence of the inhibition of the Pt catalyst complex by the vinyl groups in the system. As discussed earlier, the catalyst consists of a stable complex between Pt(0) and a di-vinyl siloxane. The mechanism involves silane transfer to the Pt complex followed by ligand exchange with the polymer double bond, activation of that bond and the subsequent addition of the silane (see **Figure 2**). In both Models 13 and 17 the chain lengths are such that the probability of the Pt complex associating with more than 1 vinyl group is low. However in Model 11 the chances of the Pt(0) complex associating with more than one vinyl at a given time is greatly increased. It is proposed that if the Pt complex does indeed associate with more than one vinyl group, it forms secondary complexes which are stable and have reduced activity towards silane transfer. Increasing the temperature will either increase the exchange rate or simply disrupt the complexation (dependent on the nature of the complex formed) but in either case serves to activate the system once more to silane transfer and vinyl addition. This is illustrated in **Figure 14**.

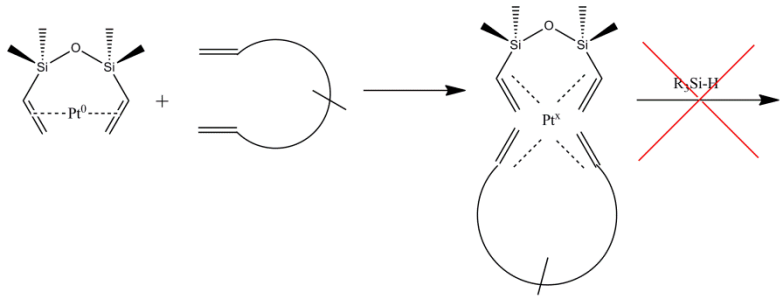

Figure 14. Proposed mechanism of Pt catalyst complex inactivation by an oligomeric vinyl terminated silicone

The origin of the fast relaxing component is a matter of some speculation, as noted in the discussion - was only partially observed and is therefore not fully captured in the data analysis. However, the consistent trend as a function of measurement time and the exceedingly short T_2 values suggest either the formation of a highly rigid crystalline component (which is unlikely in these systems) or the paramagnetic interaction of a metallic species such as Pt(IV) with the polymer system. A color change was also observed to accompany this in-growth process in Model 11 and over time the sample changed from clear to a

deep orange-yellow color, which is consistent with the presence of Pt(II) or Pt(IV) complexes. It is therefore possible that this observed process is a consequence of destabilization or other alteration of the catalyst complex within this system and indeed there is precedent for such processes in the literature (*46,50*). However, in the absence of more data, these observations must remain a somewhat speculative if not interesting aspect of this study and a subject of further work.

Conclusions

In this work it has been demonstrated that even comparatively 'simple' end-linked silane-vinyl addition cured PDMS networks have complex and non-ideal network formation chemistries that are governed by a range of factors including local availability of reactive functionalities, precursor molar mass, catalyst inhibition and complexation effects. NMR has been demonstrated to be a highly effective, informative and versatile tool for the analysis of both static network structure and real time measurements of network formation processes. The results of this study have highlighted the underlying complexity of these widely used addition cure chemistries in simple siloxane architectures and these data demonstrate that in this class of system, a silane excess is required for the formation of a fully dense and homogenous network structure. This study has also shown that network formation processes in these systems are not solely governed by functional group concentration, species diffusion and mobility – but by a complex and not fully understood series of interactions between the platinum catalyst and the vinyl groups of the polymer system itself.

Acknowledgements

This work performed under the auspices of the U.S. Department of Energy by Lawrence Livermore National Laboratory under Contract DE-AC52-07NA27344.

References

(1) Arkles, B. *Chemtech* **1983**, *13*, 542.
(2) Clarson, S. J.; Owen, M. J.; Smith, S. D. *Abstracts of Papers of the American Chemical Society* **2009**, *238*.
(3) Liu, C. *Advanced Materials* **2007**, *19*, 3783.

(4) Yoda, R. *Journal of Biomaterials Science-Polymer Edition* **1998**, *9*, 561.
(5) E., M. J.; R., A. H.; R., W. *Inorganic Polymers*; Oxford University Press: New York, 2005.
(6) Chien, A.; Maxwell, R.; Chambers, D.; Balazs, B.; LeMay, J. *Radiation Physics and Chemistry* **2000**, *59*, 493.
(7) Lewicki, J. P.; Maxwell, R. S.; Patel, M.; Herberg, J. L.; Swain, A. C.; Liggat, J. J.; Pethrick, R. A. *Macromolecules* **2008**, *41*, 9179.
(8) Traeger, R. K.; Castongu.Tt *Journal of Applied Polymer Science* **1966**, *10*, 535.
(9) Hadjoudj, A.; David, J. C.; Vergnaud, J. M. *Thermochimica Acta* **1986**, *101*, 347.
(10) Bajaj, P.; Babu, G. N.; Khanna, D. N.; Varshney, S. K. *Journal of Applied Polymer Science* **1979**, *23*, 3505.
(11) Lewicki, J. P.; Albo, R. L. F.; Alviso, C. T.; Maxwell, R. S. *Journal of Analytical and Applied Pyrolysis* **2013**, *99*, 85.
(12) Mayer, B. P.; Lewicki, J. P.; Weisgraber, T. H.; Small, W.; Chinn, S. C.; Maxwell, R. S. *Macromolecules* **2011**, *44*, 8106.
(13) Maxwell, R. S.; Chinn, S. C.; Alviso, C. T.; Harvey, C. A.; Giuliani, J. R.; Wilson, T. S.; Cohenour, R. *Polymer Degradation and Stability* **2009**, *94*, 456.
(14) Weisgraber, T. H.; Gee, R. H.; Maiti, A.; Clague, D. S.; Chinn, S.; Maxwell, R. S. *Polymer* **2009**, *50*, 5613.
(15) Dinh, L. N.; Mayer, B. P.; Maiti, A.; Chinn, S. C.; Maxwell, R. S. *Journal of Applied Physics* **2011**, *109*.
(16) Chinn, S. C.; Alviso, C. T.; Berman, E. S. F.; Harvey, C. A.; Maxwell, R. S.; Wilson, T. S.; Cohenour, R.; Saalwachter, K.; Chasse, W. *Journal of Physical Chemistry B* **2010**, *114*, 9729.
(17) Mark, J. E. *British Polymer Journal* **1985**, *17*, 144.
(18) Mark, J. E.; Pan, S. J. *Makromolekulare Chemie-Rapid Communications* **1982**, *3*, 681.
(19) Llorente, M. A.; Andrady, A. L.; Mark, J. E. *Journal of Polymer Science Part B-Polymer Physics* **1981**, *19*, 621.
(20) *Synthesis and properties of silicones and silicone modified materials*; Clarson, S. J.; Fitzgerald, J. J.; Owen, M. J.; Smith, S. D.; Van Dyke, M. E., Eds.; American Chemical Society, 2007.
(21) Cohen-Addad, J. P. *Siloxane Polymers*; Prentice Hall: Englewood Cliffs, N. J., 1993.
(22) Wunderlich, B. *Thermal Analysis of Polymeric Materials*; Springer Publishing: New York, 2005.
(23) *Differential scanning calorimetry—fourier transform IR spectroscopy and thermogravimetric analysis—fourier transform IR spectroscopy to differentiate between very similar polymer materials*; Provder, T.; Urban, M. W.; Barth, H. G., Eds.; American Chemical Society, 1994.
(24) Ettre, K.; Varadi, P. F. *Analytical Chemistry* **1962**, *34*, 752.

(25) Ke, B. *Journal of Polymer Science Part a-General Papers* **1963**, *1*, 1453.
(26) Patel, M.; Chinn, S.; Maxwell, R. S.; Wilson, T. S.; Birdsell, S. A. *Polymer Degradation and Stability* **2010**, *95*, 2499.
(27) Kimmich, R.; Fatkullin, N. *Nmr - 3d Analysis - Photopolymerization* **2004**, *170*, 1.
(28) Spiess, H. W. *Macromolecules* **2010**, *43*, 5479.
(29) Cohenaddad, J. P.; Viallat, A. *Polymer* **1986**, *27*, 1855.
(30) Ebengou, R. H.; Cohenaddad, J. P. *Polymer* **1994**, *35*, 2962.
(31) Folland, R.; Charlesby, A. *Radiation Physics and Chemistry* **1977**, *10*, 61.
(32) Folland, R.; Charlesby, A. *International Journal for Radiation Physics and Chemistry* **1976**, *8*, 555.
(33) Chasse, W.; Lang, M.; Sommer, J. U.; Saalwachter, K. *Macromolecules* **2012**, *45*, 899.
(34) Saalwachter, K.; Ziegler, P.; Spyckerelle, O.; Haidar, B.; Vidal, A.; Sommer, J. U. *Journal of Chemical Physics* **2003**, *119*, 3468.
(35) Maxwell, R. S.; Chinn, S. C.; Solyom, D.; Cohenour, R. *Macromolecules* **2005**, *38*, 7026.
(36) Saalwachter, K. *Progress in Nuclear Magnetic Resonance Spectroscopy* **2007**, *51*, 1.
(37) Maus, A.; Hertlein, C.; Saalwachter, K. *Macromolecular Chemistry and Physics* **2006**, *207*, 1150.
(38) Carr, H. Y.; Purcell, E. M. *Physical Review* **1954**, *94*, 630.
(39) Addad, J. P. C. *Progress in Nuclear Magnetic Resonance Spectroscopy* **1993**, *25*, 1.
(40) Mayer, B. P.; Chinn, S. C.; Maxwell, R. S.; Reimer, J. A. *Chemical Engineering Science* **2009**, *64*, 4684.
(41) Theocaris, P. S.; Ioakimidis, N. I. *Quarterly of Applied Mathematics* **1977**, *35*, 173.
(42) Provencher, S. W. *Computer Physics Communications* **1982**, *27*, 229.
(43) Weese, J. *Computer Physics Communications* **1992**, *69*, 99.
(44) Istratov, A. A.; Vyvenko, O. F. *Review of Scientific Instruments* **1999**, *70*, 1233.
(45) Hill, L. W. *Progress in Organic Coatings* **1997**, *31*, 235.
(46) Lewis, L. N.; Stein, J.; Gao, Y.; Colborn, R. E.; Hutchins, G. *Platinum Metals Review* **1997**, *41*, 66.
(47) Spiess, H. W. *Macromolecular Symposia* **2001**, *174*, 111.
(48) Slichter, C. P. *Principles of Magnetic Resonance*; 3 ed.; Springer: New York, 1996.
(49) Clauss, J.; Schmidt-Rohr, K.; Spiess, H. W. *Acta Polymerica* **1993**, *44*, 1.
(50) Lewis, L. N.; Sy, K. G.; Bryant, G. L.; Donahue, P. E. *Organometallics* **1991**, *10*, 3750.